

Published in final edited form as:

Chemistry. 2014 November 24; 20(48): 15824–15832. doi:10.1002/chem.201403943.

Tuning phenols with Intra-Molecular bond Shifted HYdrogens as diaCEST MRI contrast agents

Xing Yang^{1,‡}, Nirbhay N. Yadav^{1,2,‡}, Xiaolei Song^{1,2}, Sangeeta Ray Banerjee¹, Hannah Edelman¹, Il Minn¹, Peter C. M. van Zijl^{1,2}, Martin G. Pomper^{1,*}, and Michael T. McMahon^{1,2,*}

¹The Russell H. Morgan Department of Radiology, The Johns Hopkins University School of Medicine, 991 N. Broadway Baltimore, MD 21287 (USA)

²F. M. Kirby Research Center for Functional Brain Imaging, Kennedy Krieger Institute, 707 N. Broadway Ave. Baltimore, MD 21287 (USA)

Abstract

We characterize what the optimal exchange properties are for CEST contrast agents on 3T clinical scanners using CW saturation transfer, and demonstrate that the exchangeable protons in phenols can be tuned to reach these criteria through proper ring substitution. Systematic modification allows the chemical shift of the exchangeable protons to be positioned between 4.8 ppm to 12 ppm from water and enables adjustment of the proton exchange rate to maximize CEST contrast at these shifts. In particular, 44 hydrogen-bonded phenols are investigated for their potential as CEST MRI contrast agents and the stereoelectronic effects on their CEST properties summarized. Furthermore, we identify a pair of compounds, 2,5-dihydroxyterephthalic acid (**42**) and 4,6-dihydroxyisophthalic acid (**43**), which produce the highest sensitivity through incorporating two exchangeable protons per ring.

Keywords

CEST; IM-SHY; molecular imaging; MRI; contrast agents

Introduction

Due to its exquisite soft tissue contrast and high spatial resolution, magnetic resonance imaging (MRI) is a pre-eminent clinical diagnostic tool. In over one third of clinical MRI scans, exogenous contrast agents such as gadolinium complexes are administered to improve sensitivity [1]. Those compounds work by enhancing the water relaxation (T_1) in tissue, with ongoing efforts in the design of analogs that enhance relaxivity at high fields [2]. Relaxation-based agents, including gadolinium complexes, manganese [3] and iron oxides [4], were the status quo for exogenous MRI contrast until Ward and Balaban suggested as an alternative using exchangeable solute protons in diamagnetic compounds to produce MRI contrast [5]. Soon after, van Zijl developed diamagnetic polymers and Sherry and Aime developed

*Michael T. McMahon, Phone: +1-443-923-9356, Fax: 1-443-923-9505, mcmahon@mri.jhu.edu, Martin G. Pomper, Phone:

+1-410-955-2789, Fax: 1-443-817-0990, mpomper@jhmi.edu.

‡These authors contributed equally.

paramagnetic agents, respectively, which could also generate contrast based on proton exchange with water.^[6] Importantly, unlike relaxation agents, such contrast can be “turned on” by selectively irradiating the labile protons using a radiofrequency pulse corresponding to the chemical shift of the exchangeable proton in the system under study. Other significant advantages of the method, termed chemical exchange saturation transfer (CEST), are that the signal of the solute molecules, which are in relatively low concentration, can be enhanced by several orders of magnitude^[7] and that the contrast produced is sensitive to environmental parameters such as temperature, pH, membrane fluidity and cation concentration^[8]. Several common natural compounds have been reported to produce significant CEST contrast including glucose, glycogen, myo-inositol, glutamate, creatine, L-arginine, glycosaminoglycans, nucleic acids and peptides^[9]. Further, to date, several human studies with administration of exogenous diamagnetic CEST agents^[10] have been reported, with more under way.

A key requirement for CEST MRI experiments is to selectively irradiate solute protons and avoid perturbing the bulk water signal. Consequently, the chemical shift frequency of the labile solute protons must be distinct from the bulk water resonance to enable their detection through saturation transfer. On the NMR chemical shift time scale, that implies the exchangeable solute protons need to be in the slow-intermediate exchange regime. i.e., the rate of exchange (k_{ex}) is preferably be less than the difference in frequency between the exchangeable solute protons and the water protons (ω):

$$\Delta\omega > k_{ex}. \quad (1)$$

The importance in balancing chemical shift and k_{ex} of the labile protons has been discussed extensively in several reviews^[7a-c]. To define properly which k_{ex} and chemical shifts are desirable for exogenous CEST contrast agents, we numerically solved the Bloch-McConnell equations^[11] for a two-pool system for a long continuous wave saturation pulse over a range of solute proton k_{ex} and chemical shifts with the results displayed at $\omega_1 = 2 \mu\text{T}$, $4 \mu\text{T}$ in Figure 1. The simulations represent imaging conditions currently feasible on 3 T clinical scanners, and show the great advantage of increasing the chemical shift beyond 4 ppm with respect to the water proton resonance, with diminishing gains occurring by ~ 12 ppm, provided that a $4 \mu\text{T}$ saturation pulse is utilized. The optimum k_{ex} is about $1,050 \text{ s}^{-1}$ for that saturation field strength. A 55% improvement could be realized should it be feasible to increase the labile proton chemical shift to 20 ppm and apply long $8 \mu\text{T}$ saturation pulses on clinical scanners, but this is currently not feasible using a clinically relevant body coil. Diamagnetic CEST (diaCEST) contrast agents such as glucose, creatine and other common metabolites are very attractive biomarkers. However, their exchangeable protons fall within 3.6 ppm from bulk water, which as shown in Fig. 1 results in reduced sensitivity at 3 T through saturation transfer. Further shifted labile protons (up to ~ 6 ppm) have been reported in barbituric acid^[5], iopamidol analogues^[12] and thymidine analogues^[13], and represent improvements, but as shown by these simulations are still not ideal.

We are interested in developing large chemical shift diaCEST contrast agents in order to enable CEST imaging on clinical scanners. We reported previously that the intra-molecular

hydrogen bond in salicylic acid (**1**) helped to shift its phenol CEST signal to 9.3 ppm^[14]. Prolonged retention of the exchangeable phenolic proton through intra-molecular hydrogen bonding resulted in an k_{ex} of 600 s⁻¹ at neutral pH. At pH values between 6.5 and 7.4, salicylic acid gave the ideal k_{ex} (2,400 – 400 s⁻¹) for imaging at low saturation power. Its far down field chemical shift and optimum k_{ex} at neutral pH is a combination effect from hydrogen bonding strength, phenolic proton pKa, aromatic deshielding and water solvation of the exchangeable protons. In order to understand the role of these factors, we systematically investigate how chemical structure can affect the CEST properties of hydrogen bonded, phenol-based Intra-Molecular bond-Shifted HYdrogens (IM-SHY) diaCEST agents. Forty-four related compounds, which adhere to the general scaffold shown in Scheme 1, are characterized with the factors that enable optimization for CEST for this series are also summarized.

Results and Discussion

Based on the CEST properties of salicylic acid **1**, we became interested in developing a coherent strategy to refine the basic phenol scaffold to maximize the sensitivity of this class of CEST contrast agents. As the intra-molecular hydrogen bond is a key feature, we were particularly interested in investigating the influence of the hydrogen bond acceptor on the phenol protons. To measure the k_{ex} we performed QUESP^[11] measurements at 17.6 T, the highest field scanner at our institution, where the slow-to-intermediate exchange condition holds for the most compounds. Eight different intra-molecular hydrogen bond acceptors were characterized for water soluble phenols in Table 1. Compound **1** showed a k_{ex} of 410 s⁻¹, which is slightly different from our earlier reported number at neutral pH. The k_{ex} on phenol (**2**) proved too fast to allow detection through saturation transfer (Table 1), and was estimated to be > 40,000 s⁻¹ at 5.0 ppm. Changing **1** to its glycine conjugate, salicyluric acid (**3**), gave no contrast at 9.3 ppm, presumably because k_{ex} is too fast (Table 1). The amide proton also did not give significant contrast due to its slow exchange. *o*-Nitrophenol (**4**) and 8-hydroxylquinoline *N*-oxide (**5**), which were reported to form strong intra-molecular hydrogen bonds,^[15] failed to produce significant contrast (Table 1) as well. Water soluble salicylaldehyde and its derivatives were also investigated. 3-Formyl-4-hydroxybenzoic acid (**6**) and salicylaloxime (**7**) exchanged too fast to provide contrast. Interestingly, imine groups could attenuate the k_{ex} of phenol to a detectable level. *N,N'*-bis(4-carboxysalicylidene)-1,2-diaminoethane (**8**) resonated at 7.8 ppm, although the k_{ex} was still quite fast at 16,000 s⁻¹. Salen ligands such as **8** are commonly used as metal chelators and are widely applied in catalysis^[16]. Their IM-SHY signals could potentially be applied for cation sensing, because the phenol protons would be exchanged upon formation of a metal complex. Tetrazole (**9**), which is commonly used as an isostere for the carboxylate function, was also studied, but failed to provide any contrast due to excessively rapid exchange. The results suggest that the success of salicylic acid is due to the balance of the intra-molecular hydrogen bond strength and solvation by water. The carboxylate anion in salicylic acid at neutral pH helped to shift the IM-SHY proton further downfield relative to phenol (and water) while maintaining a k_{ex} appropriate for detection, while other acceptors were either too strong or weak for providing significant contrast.

After accumulating the data in Table 1, we further studied the stereo-electronic effects of aromatic ring substitution on salicylic acid. We started with an investigation of substitution at the 4- and 5-positions (Table 2). Most inductive electron donating (hydroxyl-, amino-) and withdrawing (chloro-, carboxyl-, sulfonyl- and nitro-) groups did not dramatically change the contrast at those positions (Table 2, compounds **10-14** and **16-18**). The electronic effects on the IM-SHY phenol proton were clearly reflected on the chemical shift of the peak CEST signal. 2,5-Dihydroxybenzoic acid (**10**) and 5-aminosalicylic acid (**11**) with electron donating groups *para* to the position of the IM-SHY proton showed peak signals at 8.5 ppm, compared with the 9.3 ppm in salicylic acid (**1**), which also resulted in higher pKa values. (Table 2) Electron withdrawing groups in the *para*-position (Table 2) and *meta* inductive substitutions (Table 2, compounds **16-18**) shifted the IM-SHY signal slightly downfield, which also resulted in lower pKa values. 3,5-Dinitrosalicylic acid (**15**) failed to give any contrast, because it exists predominantly in its deprotonated form at neutral pH. In contrast to the clear trend in chemical shift, the k_{ex} of IM-SHY protons were quite similar to salicylic acid at neutral pH, which indicated the carboxylate anion helped to buffer the moderate pKa changes (Table 2, compounds **10-13** and **16-18**). In the case of 5-nitrosalicylic acid (**14**) and 2-hydroxy-4-nitrobenzoic acid (**19**), the phenol proton exchanged faster at $6,000 \text{ s}^{-1}$ and $1,440 \text{ s}^{-1}$ respectively, which indicated their pKa's are quite close to the limit and the O-H bond is quite weak at neutral pH (Table 2). Assuming $\omega \sim 11 \pi \mu$, for $B_0 = 3 \text{ T}$ this translates to $k_{\text{ex}} < 1,400 \text{ s}^{-1}$. The chemical shift observed for 5-nitrosalicylic acid (**14**) was 10.3 ppm and it was close to the maximum that could be achieved by tuning only the pKa of R2-OH.

With improved understanding of the pure electronic effects on the IM-SHY signal, we investigated more complicated 3- and 6-substituted 2-hydroxybenzoic acids, which produce ortho effects on the core hydroxyl and carboxylate substituents. As shown in Table 3, substitution at the 6-position results in a more nuanced behavior. Any subtle stereo bulky modification can produce a dramatic change in the hydrogen bonding between the carboxylate and IM-SHY proton. Although 2-hydroxy-1-naphthoic acid (**20**) (Table 3) and 6-methoxysalicylic acid (**21**) (Table 3) still gave IM-SHY contrast at 9.5 ppm and 9.0 ppm, the k_{ex} were around 11-12 times faster compared with salicylic acid, making them less useful for low field MR applications. Interestingly, 2,6-dihydroxybenzoic acid (**22**) (Table 3) with two O-H hydrogen-bonded to the carboxylate anion, exchanged with water at the slow rate of 30 s^{-1} . That result seems to suggest the importance of the solvation of the carboxylate on buffering the IM-SHY k_{ex} . Overall, these results indicate that the k_{ex} can be dramatically altered by substituting at the 6-position without altering the chemical shift.

In contrast to the 6-position, 2-hydroxybenzoic acids with 3-position substituents can give higher chemical shift than salicylic acid (**1**) with tunable k_{ex} . 3-Methylsalicylic acid (**23**) (Table 4) showed peak contrast at 9.5 ppm at a slightly slower k_{ex} of 240 s^{-1} , compared to 410 s^{-1} for **1**. Increasing the size of the substituent at the 3-position likely would prevent access to water needed for solvation, and the phenol proton in 3,5-di-tert-butylsalicylic acid (**24**) (Table 4) exchanged with water slowly at 9.3 ppm (21 s^{-1}). 3-Halo substitution affected the IM-SHY signal through a combination of steric and electronic de-shielding effects. The electronic de-shielding trend was shown clearly changing from fluoro to chloro, bromo and

iodo, with an increase in the size of the polarizable electron cloud. The chemical shifts were observed at 9.5, 10.3, 10.5 and 10.8 ppm respectively. (Table 4, compounds **25-28**) The combination of steric and electronic de-shielding effects was reflected in the drop in k_{ex} from 980, to 550 and 290 s^{-1} . 3,5-Dibromosalicylic acid (**27**) proved to be the optimum with both a large chemical shift and suitable k_{ex} for low field power MR imaging.

3-Aryl substituted salicylic acids were also studied. 1-Hydroxy-2-naphthoic acid (**29**) did possess a larger chemical shift at 10.5 ppm, but the k_{ex} dropped to 220 s^{-1} , from introduction of extra steric factors (Table 4). In 8-hydroxy-7-quinolinecarboxylic acid (**30**), the carboxylate anion was less effective in attenuating the k_{ex} of the phenolic proton and the k_{ex} was 1,400 s^{-1} at a chemical shift of 10.3 ppm. A reasonable explanation might be that the presence of hydrogen bonding of the quinoline nitrogen to water, inducing a faster proton k_{ex} (Table 4), although solvation could also play a role. That is similar to behavior seen for amide protons near lysine or arginine sidechains in small peptides [9h]. A similar effect was also observed in 2,3-dihydroxybenzoic acid (**31**), which resonated at 9.0 ppm with an k_{ex} of 2,200 s^{-1} (Table 4). In contrast, its close analogue, 3-methoxysalicylic acid (**32**), demonstrated the expected IM-SHY signal at 9.3 ppm and 440 s^{-1} (Table 4). However, in 3-aminosalicylic acid (**33**), that acceleration effect was not observed with the k_{ex} 400 s^{-1} (Table 4). The effect of electron withdrawing groups was also studied. 3-Formylsalicylic acid (**34**) generated CEST signal at 10.5 ppm with a k_{ex} of 520 s^{-1} , but 2-hydroxyisophthalic acid (**35**) had a higher k_{ex} at 7,100 s^{-1} , decreasing available signal (Table 4). The largest de-shielding effect was achieved on 3-nitrosalicylic acid (**36**), with the OH resonating at 12.0 ppm, the farthest we have measured for any diaCEST probe, with a moderate k_{ex} of 1,400 s^{-1} (Table 4).

A remaining issue to consider is the role of the phenolic O-H group in 2-hydroxybenzoic acid. We have identified a series of N-H groups as alternatives, including: arylamino (4.8 ppm for compound **37**), sulfonamido (6.3-7.8 ppm for compounds **38-40**) and trifluoroacetamido (9.3 ppm for compound **41**) groups [17] (Table 5). They behaved in a tunable and pH independent manner as described previously, complementary to the 2-hydroxybenzoic acids discussed here.

Our current understanding of the CEST properties of the 2-hydroxybenzoic acid scaffold are summarized in Scheme 2. A) The carboxylate anion is critical to buffer the proton k_{ex} of the ortho phenol. It provides the hydrogen bonding and appropriate water solvation environment around the exchangeable proton. B) Substitutions at the 4- and 5- positions on 2-hydroxybenzoic acid slightly affect the chemical shift through electronic effects. Those normally do not change the k_{ex} significantly, with the exception of the 5-nitro and 4-nitro groups. They present the best positions at which to conjugate targeting agents and other functions while maintaining CEST signal. C) Modification of the 6-position is not suggested. Maintenance of a R-6 proton is required to provide the correct k_{ex} for low field CEST imaging. D) The 3-position is less predictable. Bulky modification at R-3 can reduce the k_{ex} but fast exchangeable proton substitutions, such as O-H and pyridinium can also be introduced to increase k_{ex} and also extra de-shielding can be introduced through modification of the R-3 position with bromo, iodo, aryl, carbonyl and nitro groups. It is the

ideal position to design smart, switchable IM-SHY probes. E). The R-2-OH group could be switched to several N-H groups.

With the basic properties of IM-SHY 2-hydroxybenzoic acid probes discussed above, we decided to investigate if we could improve the detection limit further through increasing the number of IM-SHY cores. To avoid the ortho substitution close to the primary IM-SHY core, 2,5-dihydroxyterephthalic acid (**42**) and 4,6-dihydroxyisophthalic acid (**43**) were tested (Table 6). Both of those compounds performed extremely well as high sensitivity diaCEST probes. 2,5-Dihydroxyterephthalic acid (**42**) IM-SHY protons resonated at 8.3 ppm with k_{ex} of 980 s^{-1} , making it a higher sensitivity probe when high saturation fields ($4\text{ }\mu\text{T}$) are employed. 4,6-Dihydroxyisophthalic acid IM-SHY protons resonated at 9.8 ppm and exchanged with water at 460 s^{-1} , making this compound suitable for use at lower magnetic field strengths ($2\text{ }\mu\text{T}$). They can generate 17.1 % and 13.0 % contrast respectively, at 10 mM concentration using $3.6\text{ }\mu\text{T}$, the best of any diaCEST agents evaluated. Pamoic acid (**44**), a FDA proved drug additive [18], was also tested. But the IM-SHY protons exchanged too slowly (130 s^{-1}), producing only 5.7 % contrast at 10 mM, because of the bulky ortho substitution to the phenolic O-H.

We decided to test the detection limit of the agent generating the highest contrast, 2,5-dihydroxyterephthalic acid (**42**), at 3T to determine whether it could be applied easily to scanning at clinical field strengths. Below 10 mM, the contrast was linearly dependent on concentration, as shown in Figure 2. At $2.1\text{ }\mu\text{T}$, 0.5 mM of **42** still produced 0.6 % contrast at 8.5 ppm, as shown in Figure 2. The deviation between simulation and experiment for the 10 mM concentration found at $\sim 1\text{ ppm}$ are most likely due to imperfect B_0 correction. Because of its higher k_{ex} at $T=37\text{ }^\circ\text{C}$, the detection limit could be pushed down to 0.2 mM with around 0.5 % contrast when using $8\text{ }\mu\text{T}$ (See supporting information). This detection threshold is dependent on the experimental conditions of the scanner and application.

Hydrogen bonded phenols exist widely as natural products and also as therapeutics. For example, aspirin is the most commonly used nonsteroidal anti-inflammatory drug (NSAID), which works as a prodrug of salicylic acid. Doxorubicin and mitoxantrone are used commonly as anti-tumor drugs. Tetracycline is one of the oldest antibiotics. Enterobacin exists as the strongest iron binding compound in bacteria. The toxicity for a number of those compounds has been determined, and they are generally not toxic at doses suitable for diaCEST imaging. For example, 4-amino salicylic acid has a median LD_{50} of 4,250 mg/kg. 2,4-Dihydroxy benzoic acid, salicylic acid, flufenamic acid also have relatively high LD_{50} values at 800 mg/kg, 500 mg/kg and 150 mg/kg, respectively. As described above, we define criteria that enable phenols to produce substantial CEST contrast at 3 T, which involve a balance between chemical shift and water k_{ex} . As shown in Figure 3, compounds were identified that produce strong contrast from 4.8 ppm to 12 ppm from water based on modifications at the R3, R4, R5, R6 positions in addition to modification of the OH hydrogen bonding partner.

Lanthanide, Iron, Cobalt and Nickel complexes can also feature exchangeable protons with large chemical shifts from water (on the order of 30-700 ppm) and suitable k_{ex} [7a, 19]. The large chemical shift difference with water for those paramagnetic CEST (paraCEST) agents

enables faster exchange while adhering to the slow-intermediate exchange condition mentioned in Eq. 1 (e.g. axial water ligands exchanging with bulk water). Despite the advantages of the larger allowed k_{ex} , the contrast produced by all CEST agents will be limited using when utilizing a 4 μ T continuous wave saturation field. Larger contrast could therefore be realized using transmission coils capable of keeping the Specific Absorption Rate (SAR) produced by long $> 8 \mu$ T pulses to within heating limits.

While we have concentrated on the performance of the IM-SHY scaffold using continuous wave saturation transfer preparation, the measurements included do not represent the performance of these compounds using pulsed exchange transfer methods such as two frequency irradiation [20], CERT [21], Frequency labeled EXchange transfer (FLEX)[22] or Variable Delay Multiple Pulse (VDMP) transfer [23] as these sequences are still under development at 3T. The use of a limited series of short selective high-power pulses has advantages for detecting rapidly exchanging compounds [7d] as recently demonstrated using FLEX on a paraCEST agent with a water k_{ex} of 19,000 Hz. That will be the subject of future studies. It is expected that the set of compounds described here will perform well using these new schemes.

Conclusion

In conclusion, a general scaffold for producing strong CEST contrast is described based on analysis of 44 analogs of 2-hydroxybenzoic acid. Stereoelectronic effects of substitutions on the aromatic ring on CEST properties are summarized, with the phenol IM-SHY agents producing strong contrast from 4.8 ppm to 12 ppm. Compounds can be tuned with respect both to their pK_a values and proton k_{ex} , the key determinants of CEST signal by enabling control of chemical shift and degree of water saturation, which impact on overall sensitivity. These probes were designed with multi-frequency CEST imaging in mind, with frequencies spanning a range that should allow discrimination between multiple agents within an image. As small molecules, we identify **42** and **43** as the highest sensitivity contrast agents through incorporating two IM-SHY protons with suitable k_{ex} and could be detected down to 200 μ M for **42** at clinically useful field strengths.

Experimental Section

Phantom Preparation

Salicylic acid, phenol, 2-nitrophenol, 8-hydroxylquinoline N-oxide, 5-formyl-salicylaldehyde, 2,5-dihydroxybenzoic, 5-amino-salicylic acid, 5-chlorosalicylic acid, 5-nitrosalicylic acid, 2,4-dihydroxybenzoic acid, 4-aminosalicylic acid, 3,5-dinitrosalicylic acid, 4-hydroxyisophthalic acid, 2-hydroxy-1-naphthoic acid, 2-hydroxy-6-methoxybenzoic acid, 2,6-dihydroxybenzoic acid, 3-methylsalicylic acid, 2,4-di-tert-butyl-6-hydroxybenzoic acid, 2,4-dichloro-6-hydroxybenzoic acid, 2,4-dibromo-6-hydroxybenzoic acid, 2-hydroxy-4,6-diiodobenzoic acid, 1-hydroxy-2-naphthoic acid, 8-hydroxyquinoline-7-carboxylic acid, 2,3-dihydroxybenzoic acid, 2-hydroxy-3-methoxybenzoic acid, 3-amino-2-hydroxybenzoic acid and 3-formyl-2-hydroxybenzoic acid were purchased from Sigma Aldrich (St. Louis, MO). 2-hydroxy-5-sulfobenzoic acid, 3-fluorosalicylic acid, 2,5-dihydroxyterephthalic acid and Pamoic acid were purchased from TCI America (Portland,

OR). Salicylaldoxime, 2-(1H-tetrazol-5-yl) phenol and 3-methoxysalicylic acid were purchased from Alfa Aesar (Ward Hill, MA). Salicyluric acid was purchased from SynQuest Labs Inc. (Alachua FL). 4-Nitrosalicylic acid was purchased from Chem-Impex Inc.(Wood Dale, IL). 3-nitrosalicylic acid was purchased from Combi-Blocks Inc.(San Diego, CA). 2-Hydroxyisophthalic acid was purchased from Sinova Inc. (Bethesda, MD). 4,6-dihydroxyisophthalic acid was purchased from J&W Pharmed LLC(Levittown, PA).

Samples were dissolved in 0.01 M phosphate-buffered saline (PBS) at concentrations from 0.1 mM to 10 mM, and titrated using high concentration HCl/NaOH to obtain physiologically relevant pH values ~7.4. The solutions were placed into 1 mm glass capillaries and assembled in a holder for CEST MR imaging.

Data acquisition

Phantom CEST experiments were performed on a Bruker Avance III 17.6 T vertical bore MR scanner using a 20 mm SAW type microimaging transmit/receive coil. The samples were kept at 37 °C during imaging. CEST images were acquired using a RARE (RARE factor = 32) sequence with a continuous wave (CW) saturation pulse length of 6 s and saturation field strengths of 1.0, 3.6, and 8.0 μ T. The CEST Z-spectra were acquired by incrementing the saturation frequency every 0.25 ppm from -15.0 to 15.0 ppm. TR = 15 s, TE = 8 ms, matrix size = 64 \times 32, slice thickness = 3 mm.

For compound 42, CEST experiments were also performed on a 3.0 T Philips Medical Systems human MRI scanner using a parallel transmit body coil for RF transmission and a 32-channel head coil for reception. The CEST images were acquired using a Turbo Spin echo sequence with a CW saturation pulse length of 3 s. The CEST Z-spectra were acquired by incrementing the saturation frequency every 0.38 ppm from -15.0 to 15.0 ppm. TR = 12 s, TE = 6.4 ms, matrix size = 64 \times 58, slice thickness = 10 mm.

Post-processing

CEST contrast was quantified using MTR_{asym} [24]

$$MTR_{asym}(\omega) = [S_{sat}(-\omega) - S_{sat}(\omega)] / S_0.$$

Prior to performing MTR_{asym} , the effects from B_0 variations were corrected for using the WASSR [25] method.

Acknowledgments

Funding was provided by NIH R01 EB012590, R01 EB015031, R01 EB015032, U54CA151838, S10RR025118, K25CA148901.

Dedicated to John A. Katzenellenbogen on the occasion of his 70th birthday.

References

1. Caravan P, Ellison JJ, McMurry TJ, Lauffer RB. Chemical Reviews. 1999; 99:2293–2352. [PubMed: 11749483]

2. a) Caravan P, Farrar CT, Frullano L, Uppal R. *Contrast Media & Molecular Imaging*. 2009; 4:89–100. [PubMed: 19177472] b) Livramento JB, Helm L, Sour A, O'Neil C, Merbach AE, Toth E. *Dalton Transactions*. 2008:1195–1202. [PubMed: 18283380]
3. Pautler RG, Silva AC, Koretsky AP. *Magnetic Resonance in Medicine*. 1998; 40:740–748. [PubMed: 9797158]
4. a) Laurent S, Forge D, Port M, Roch A, Robic C, Elst LV, Muller RN. *Chemical Reviews*. 2008; 108:2064–2110. [PubMed: 18543879] b) Harisinghani MG, Barentsz J, Hahn PF, Deserno WM, Tabatabaei S, van de Kaa CH, de la Rosette J, Weissleder R. *New England Journal of Medicine*. 2003; 348:2491–U2495. [PubMed: 12815134]
5. Ward KM, Aletras AH, Balaban RS. *Journal of Magnetic Resonance*. 2000; 143:79–87. [PubMed: 10698648]
6. a) Zhang S, Winter P, Wu K, Sherry AD. *Journal of the American Chemical Society*. 2001; 123:1517–1518. [PubMed: 11456734] b) Aime S, Delli Castelli D, Terreno E. *Angewandte Chemie*. 2002; 114:4510–4512. c) Goffeney N, Bulte JW, Duyn J, Bryant LH Jr, van Zijl PC. *Journal of the American Chemical Society*. 2001; 123:8628–8629. [PubMed: 11525684]
7. a) Hancu I, Dixon WT, Woods M, Vinogradov E, Sherry AD, Lenkinski RE. *Acta Radiologica*. 2010; 51:910–923. [PubMed: 20828299] b) Liu GS, Song XL, Chan KWY, McMahon MT. *Nmr in Biomedicine*. 2013; 26:810–828. [PubMed: 23303716] c) Castelli DD, Terreno E, Longo D, Aime S. *Nmr in Biomedicine*. 2013; 26:839–849. [PubMed: 23784956] d) van Zijl PCM, Yadav NN. *Magnetic Resonance in Medicine*. 2011; 65:927–948. [PubMed: 21337419]
8. a) Schroeder L, Meldrum T, Smith M, Lowery TJ, Wemmer DE, Pines A. *Physical Review Letters*. 2008; 100b) Ward KM, Balaban RS. *Magnetic resonance in medicine : official journal of the Society of Magnetic Resonance in Medicine / Society of Magnetic Resonance in Medicine*. 2000; 44:799–802. c) Schnurr M, Witte C, Schroder L. *Physical Chemistry Chemical Physics*. 2013; 15:14178–14181. [PubMed: 23793163] d) Trokowski R, Ren JM, Kalman FK, Sherry AD. *Angewandte Chemie-International Edition*. 2005; 44:6920–6923.
9. a) Gilad AA, McMahon MT, Walczak P, Winnard PT Jr, Raman V, van Laarhoven HW, Skoglund CM, Bulte JW, van Zijl PC. *Nature Biotechnology*. 2007; 25:217–219. b) Chan KW, Liu G, Song X, Kim H, Yu T, Arifin DR, Gilad AA, Hanes J, Walczak P, van Zijl PC, Bulte JW, McMahon MT. *Nature materials*. 2013; 12:268–275. c) Chan KW, McMahon MT, Kato Y, Liu G, Bulte JW, Bhujwala ZM, Artemov D, van Zijl PC. *Magnetic resonance in medicine : official journal of the Society of Magnetic Resonance in Medicine / Society of Magnetic Resonance in Medicine*. 2012; 68:1764–1773. d) Ling W, Regatte RR, Navon G, Jerschow A. *Proceedings of the National Academy of Sciences of the United States of America*. 2008; 105:2266–2270. [PubMed: 18268341] e) Cai K, Haris M, Singh A, Kogan F, Greenberg JH, Hariharan H, Detre JA, Reddy R. *Nature Medicine*. 2012; 18:302–306. f) Haris M, Cai K, Singh A, Hariharan H, Reddy R. *NeuroImage*. 2011; 54:2079–2085. [PubMed: 20951217] g) Kogan F, Haris M, Singh A, Cai K, Debrosse C, Nanga RP, Hariharan H, Reddy R. *Magnetic resonance in medicine : official journal of the Society of Magnetic Resonance in Medicine / Society of Magnetic Resonance in Medicine*. 2013h) McMahon MT, Gilad AA, DeLiso MA, Cromer Berman SM, Bulte JWM, van Zijl PCM. *Magnetic Resonance in Medicine*. 2008; 60:803–812. [PubMed: 18816830] i) Zhou J, Lal B, Wilson DA, Laterra J, van Zijl PC. *Magnetic resonance in medicine : official journal of the Society of Magnetic Resonance in Medicine / Society of Magnetic Resonance in Medicine*. 2003; 50:1120–1126. j) Walker-Samuel S, Ramasawmy R, Torrealdea F, Rega M, Rajkumar V, Johnson SP, Richardson S, Goncalves M, Parkes HG, Arstad E, Thomas DL, Pedley RB, Lythgoe MF, Golay X. *Nature Medicine*. 2013k) Liu GS, Liang YJ, Bar-Shir A, Chan KWY, Galpoththawela CS, Bernard SM, Tse T, Yadav NN, Walczak P, McMahon MT, Bulte JWM, van Zijl PCM, Gilad AA. *Journal of the American Chemical Society*. 2011; 133:16326–16329. [PubMed: 21919523]
10. a) Mueller-Lutz, A.; Khalil, N.; Lanzman, RS.; Oeltzschner, G.; Pentang, G.; Jellus, V.; Schmitt, B.; Antoch, G.; Wittsack, H-J. *Proc Intl Soc Mag Reson Med*. Salt Lake City UT: 2013. p. 4220b) Keupp, J.; Dimitrov, I.; Langereis, S.; Togao, O.; Takahashi, M.; Sherry, AD. *Proc Intl Soc Mag Reson Med*. Montreal, Quebec, Canada: 2011. p. 828
11. McMahon MT, Gilad AA, Zhou J, Sun PZ, Bulte JWM, van Zijl PCM. *Magnetic Resonance in Medicine*. 2006; 55:836–847. [PubMed: 16506187]

12. a) Aime S, Calabi L, Biondi L, De Miranda M, Ghelli S, Paleari L, Rebaudengo C, Terreno E. *Magnetic Resonance in Medicine*. 2005; 53:830–834. [PubMed: 15799043] b) Chen LQ, Howison CM, Jeffery JJ, Robey IF, Kuo PH, Pagel MD. *Magnetic Resonance in Medicine*. 2013:n/a–n/a.
13. Bar-Shir A, Liu GS, Liang YJ, Yadav NN, McMahon MT, Walczak P, Nimmagadda S, Pomper MG, Tallman KA, Greenberg MM, van Zijl PCM, Bulte JWM, Gilad AA. *Journal of the American Chemical Society*. 2013; 135:1617–1624. [PubMed: 23289583]
14. Yang X, Song XL, Li YG, Liu GS, Banerjee SR, Pomper MG, McMahon MT. *Angewandte Chemie-International Edition*. 2013; 52:8116–8119.
15. a) Brzezinski B, Zundel G. *Journal of Magnetic Resonance* (1969). 1982; 48:361–366.b) Abraham RJ, Mobli M. *Magnetic Resonance in Chemistry*. 2007; 45:865–877. [PubMed: 17729232]
16. a) Cozzi PG. *Chemical Society Reviews*. 2004; 33:410–421. [PubMed: 15354222] b) Tokunaga M, Larrow JF, Kakiuchi F, Jacobsen EN. *Science*. 1997; 277:936–938. [PubMed: 9252321]
17. Song X, Yang X, Ray Banerjee S, Pomper MG, McMahon MT. *Contrast Media & Molecular Imaging*. 201410.1002/cmmi.1597
18. Saesmaa T, Tötterman AMT. *Journal of Pharmaceutical and Biomedical Analysis*. 1990; 8:61–65. [PubMed: 2102266]
19. a) Terreno E, Castelli DD, Aime S. *Contrast Media and Molecular Imaging*. 2010; 5:78–98. [PubMed: 20419761] b) Yoo B, Pagel MD. *Journal of the American Chemical Society*. 2006; 128:14032–14033. [PubMed: 17061878] c) Dorazio SJ, Tsitovich PB, Sifers KE, Sperryak JA, Morrow JR. *Journal of the American Chemical Society*. 2011; 133:14154–14156. [PubMed: 21838276] d) Olatunde AO, Dorazio SJ, Sperryak JA, Morrow JR. *Journal of the American Chemical Society*. 2012; 134:18503–18505. [PubMed: 23102112] e) Dorazio SJ, Olatunde AO, Sperryak JA, Morrow JR. *Chemical Communications*. 2013; 49:10025–10027. [PubMed: 24045271]
20. Lee JS, Regatte RR, Jerschow A. *Journal of Magnetic Resonance*. 2012; 215:56–63. [PubMed: 22237631]
21. Zu ZL, Janve VA, Li K, Does MD, Gore JC, Gochberg DF. *Magnetic Resonance in Medicine*. 2012; 68:711–719. [PubMed: 22161770]
22. a) Yadav NN, Jones CK, Xu JD, Bar-Shir A, Gilad AA, McMahon MT, van Zijl PCM. *Magnetic Resonance in Medicine*. 2012; 68:1048–1055. [PubMed: 22837066] b) Friedman JI, McMahon MT, Stivers JT, Van Zijl PCM. *Journal of the American Chemical Society*. 2010; 132:1813. [PubMed: 20095603]
23. Xu J, Yadav NN, Bar-Shir A, Jones CK, Chan KWY, Zhang J, Walczak P, McMahon MT, van Zijl PCM. *Magnetic Resonance in Medicine*. 2013:n/a–n/a.
24. Guivel-Scharen V, Sinnwell T, Wolff SD, Balaban RS. *Journal of Magnetic Resonance*. 1998; 133:36–45. [PubMed: 9654466]
25. Kim M, Gillen J, Landman BA, Zhou J, van Zijl PC. *Magnetic resonance in medicine : official journal of the Society of Magnetic Resonance in Medicine / Society of Magnetic Resonance in Medicine*. 2009; 61:1441–1450.

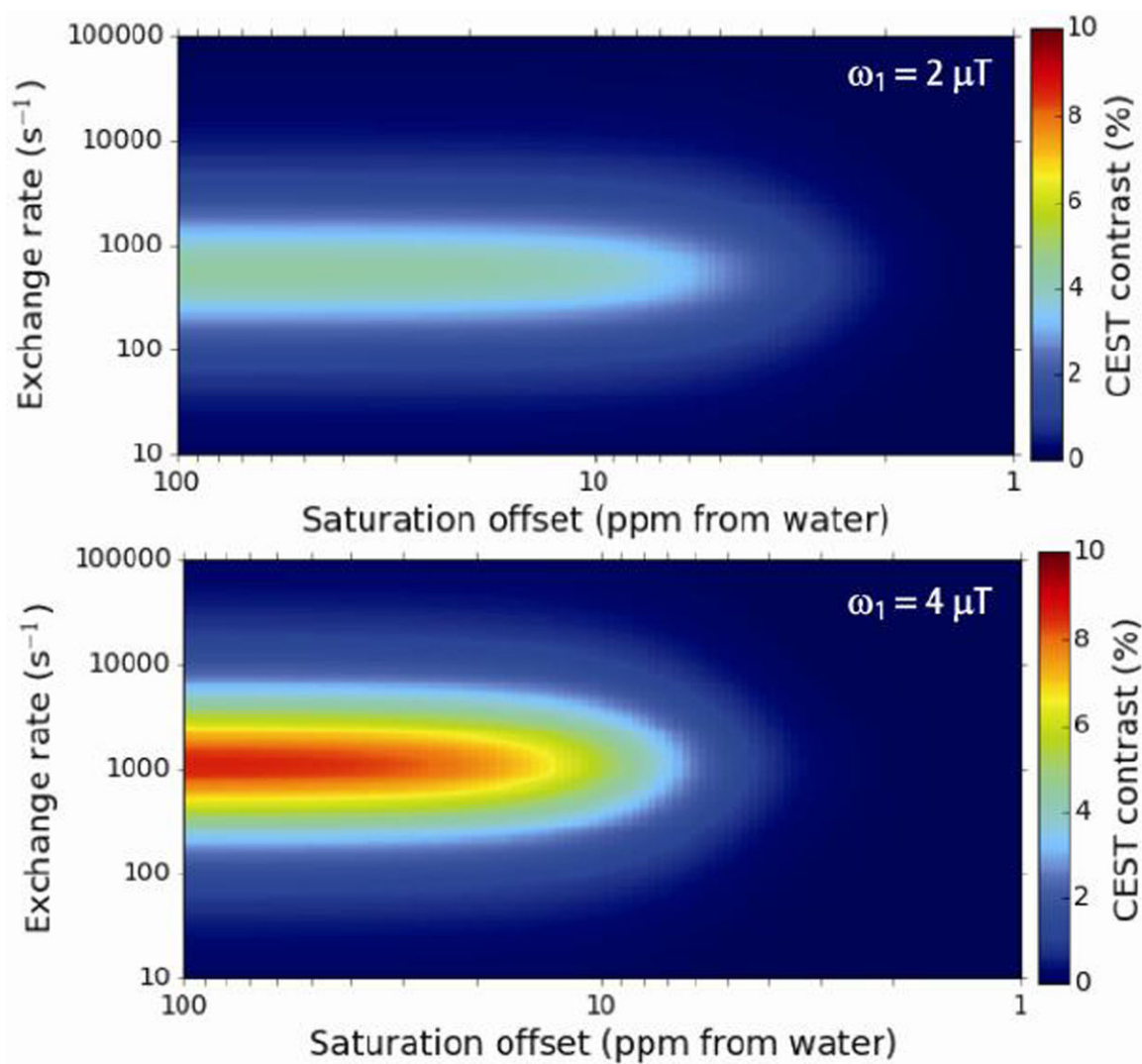


Figure 1. Simulated CEST contrast at 3T as a function of labile proton chemical shift and exchange rate

Conditions: $t_{\text{sat}} = 3 \text{ s}$, $X_{\text{CA}} = 10 \text{ mM}$, $T_{1\text{w}} = 3 \text{ s}$, $T_{2\text{w}} = 0.1 \text{ s}$, $T_{1\text{s}} = 3 \text{ s}$, $T_{2\text{s}} = 0.1 \text{ s}$, $\omega_1 = 2 \mu\text{T}$ (upper panel) $\omega_1 = 4 \mu\text{T}$ (lower panel).

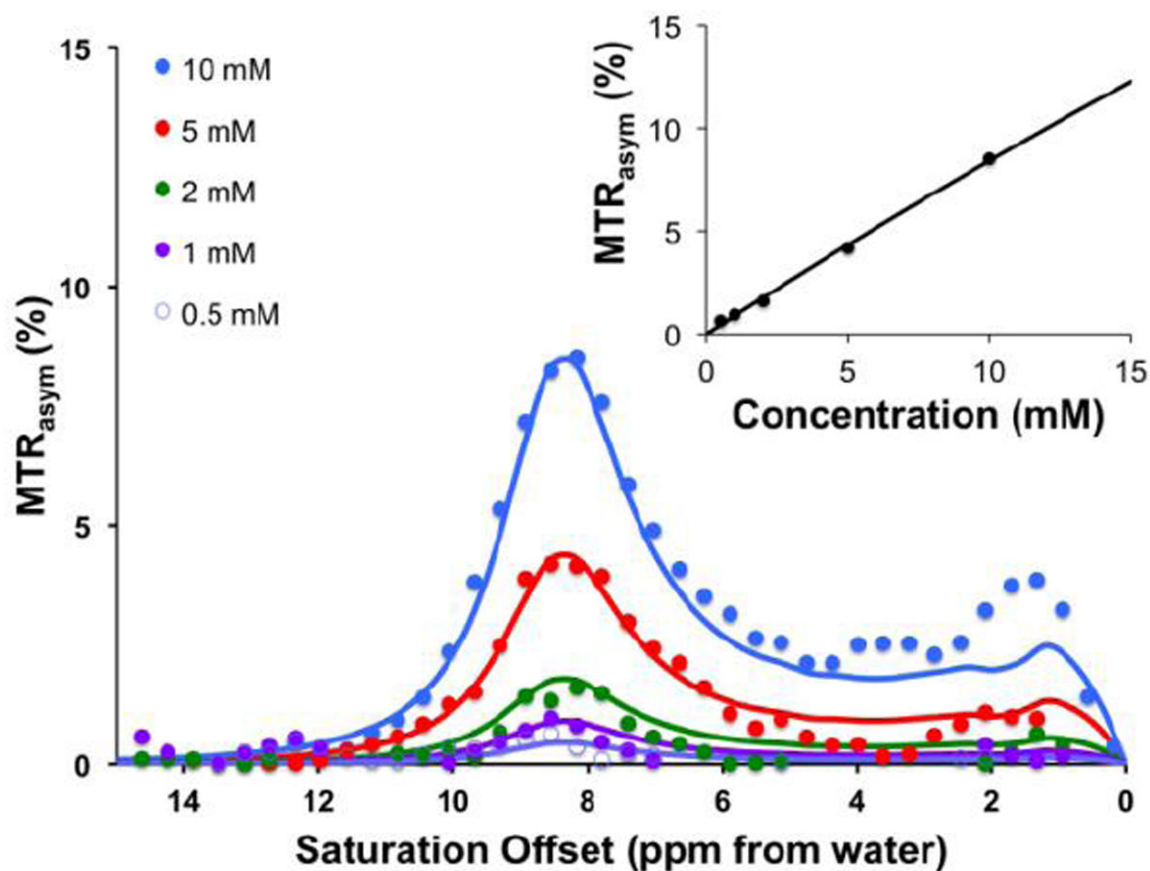


Figure 2. Concentration dependence and detection limit of 2,5-dihydroxyterephthalic acid (42) at 3 T

Conditions: CEST data were obtained at 10 mM, 5mM, 2mM, 1 mM, 0.5 mM concentrations, pH 7.3 - 7.4, $t_{\text{sat}} = 3$ sec, $\omega_1 = 2.1 \mu\text{T}$ and $T = 32^\circ\text{C}$. For the inner panel, the CEST contrast at 8.5 ppm was plotted. Experimental data are shown as closed circles, while the lines represent Bloch simulations.

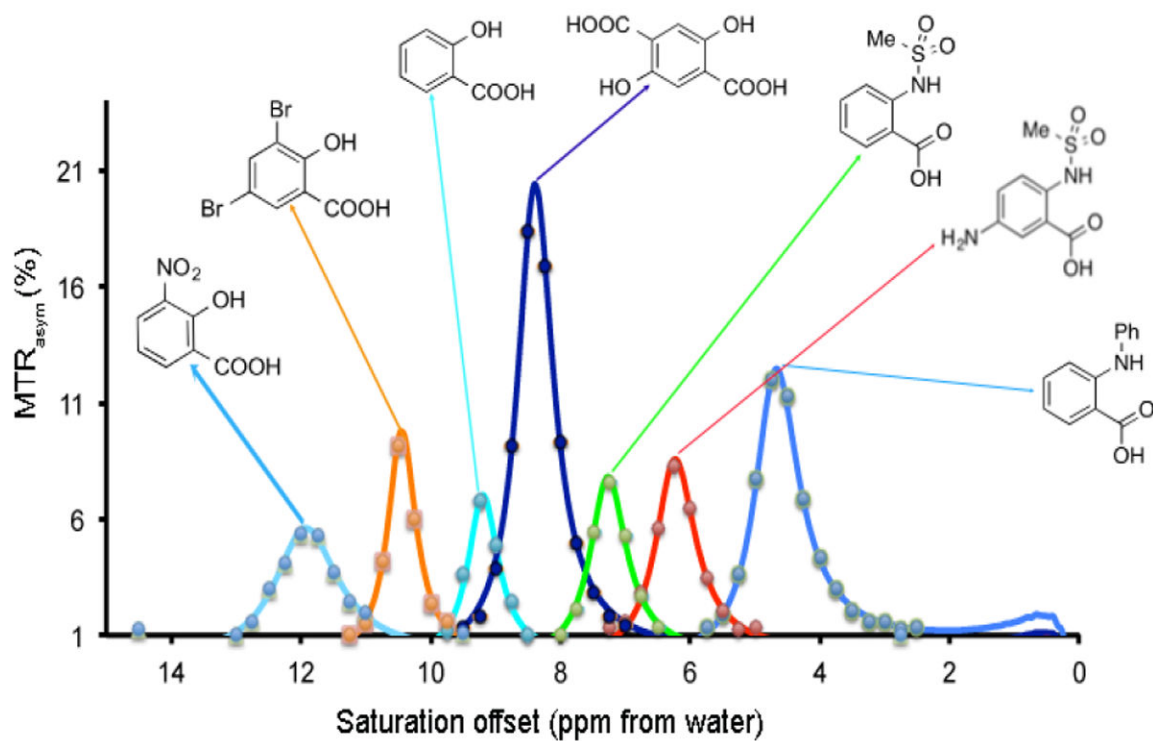
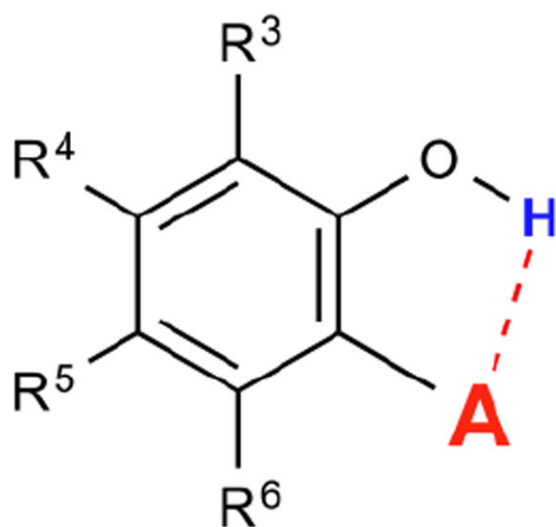


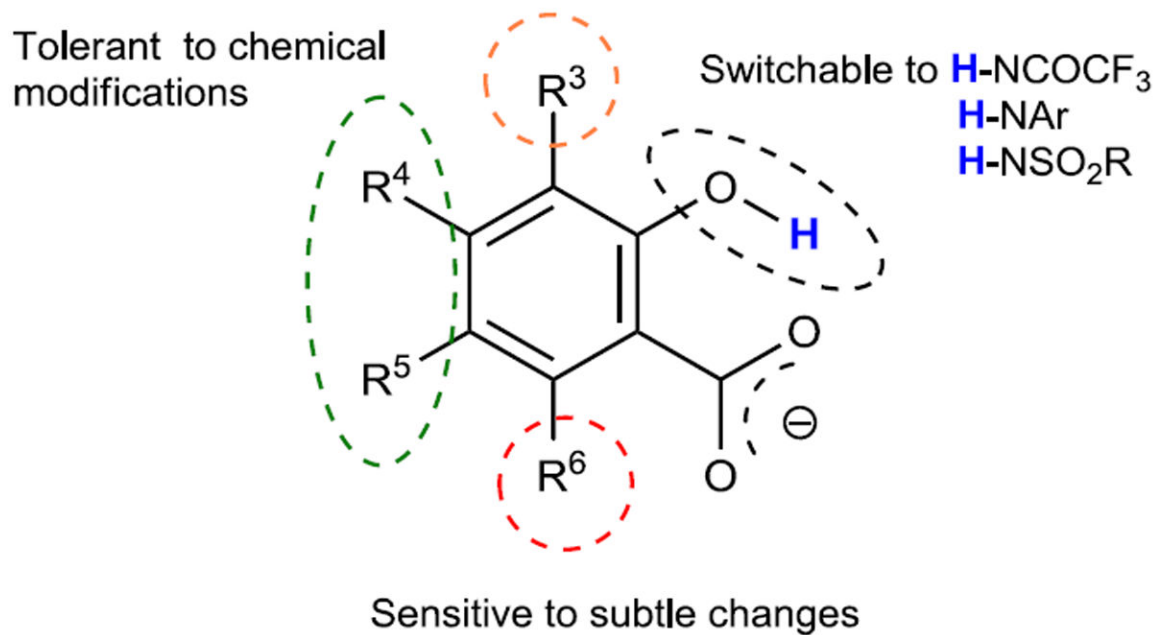
Figure 3. High performance IM-SHY agents with different exchangeable proton frequencies
 Conditions: CEST data were obtained at 17.6 T using 10 mM concentrations, pH 7.3 - 7.4, $t_{\text{sat}} = 3$ sec, $\omega_1 = 3.6 \mu\text{T}$ and $T = 37^\circ\text{C}$. Experimental data are shown as closed circles, while the lines represent Bloch simulations.



A = Hydrogen Bond Acceptor

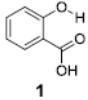
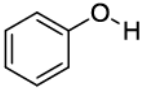
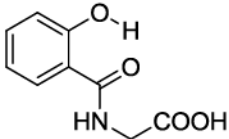
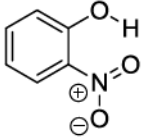
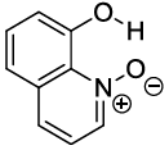
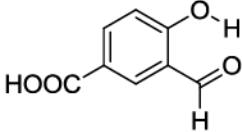
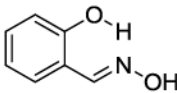
Scheme 1. General scaffold for phenol based IM-SHY CEST agents

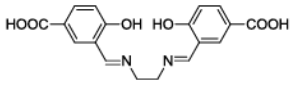
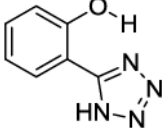
Tunable by size and de-shielding
properties of functional groups



Scheme 2. Stereo-electronic effect on the CEST properties of IM-SHY agents

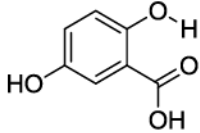
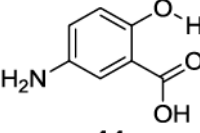
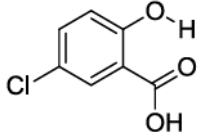
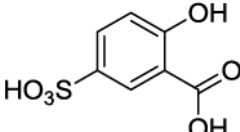
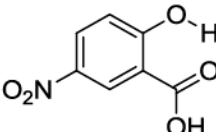
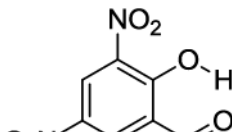
Table 1
Effect of hydrogen bond acceptor on the CEST property of phenol based IM-SHYs

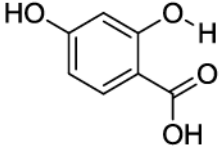
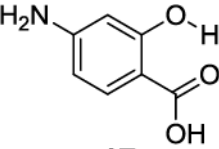
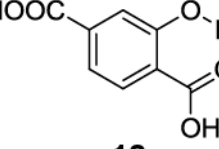
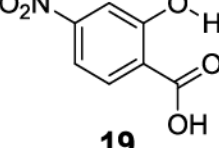
Compound	Signal (ppm)	Contrast(%)	k_{ex} (s^{-1})
 1	9.3	6.8	410±20
 2	~5.0	< 0.4	NA
 3	None	0	NA
 4	None	0	NA
 5	9.5	0.7	29±10
 6	None	0	NA
 7	None	0	NA

Compound	Signal (ppm)	Contrast(%)	k_{ex} (s^{-1})
 8	7.8	1.7	16,000±4000
 9	None	0	NA

Conditions: CEST data were obtained at 10 mM concentration, $t_{sat} = 3$ sec, $\omega_1 = 3.6$ μ T and 37 °C. Note: As discussed in an earlier section, the k_{ex} of phenol based protons drops dramatically with an increase in pH (from 6-8). The direct comparison of k_{ex} also needs to take this into account. All pH values in this paper were titrated to 7.3 - 7.4 for consistency.

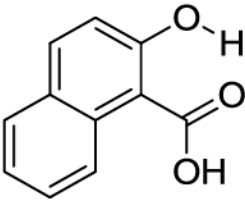
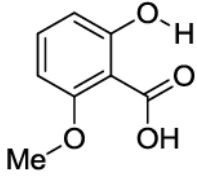
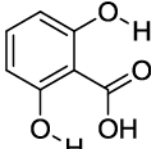
Table 2
Electronic effect of 4- and 5- substituted 2-hydroxybenzoic acids

Compound	Signal (ppm)	Contrast(%)	k_{ex} (s^{-1})
 <p>10</p>	8.5	7.7	410±30
 <p>11</p>	8.5	7.0	370±20
 <p>12</p>	9.0	6.2	260±40
 <p>13</p>	9.5	5.7	320±30
 <p>14</p>	10.3	3.1	6000±1000
 <p>15</p>	None	0	NA

Compound	Signal (ppm)	Contrast(%)	k_{ex} (s^{-1})
 16	9.5	7.2	450±30
 17	9.5	6.6	360±30
 18	9.3	6.7	420±20
 19	9.5	6.7	1440±70

Conditions: CEST data were obtained at 10 mM concentration, pH 7.3 - 7.4, t_{sat} = 3 sec, ω_1 = 3.6 μ T and 37 °C.

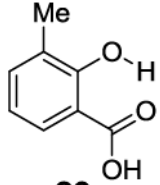
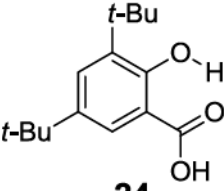
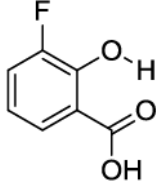
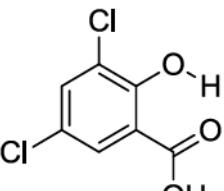
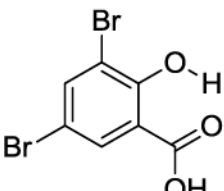
Table 3
Stereo-electronic effect of 6-substituted 2-hydroxybenzoic acids

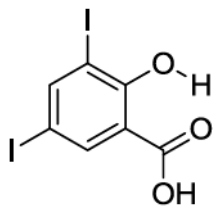
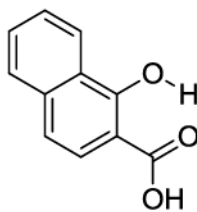
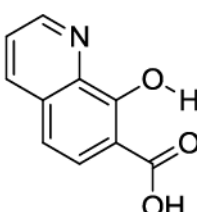
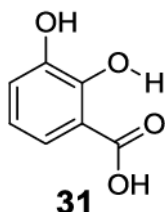
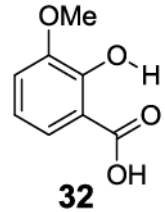
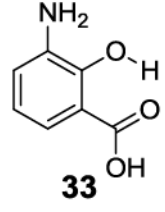
Compound	Signal (ppm)	Contrast(%)	k_{ex} (s^{-1})
 20	9.5	3.4	4800±700
 21	9.0	3.2	4900±600
 22	9.3	0.4	30±10

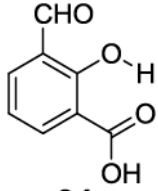
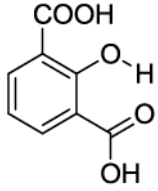
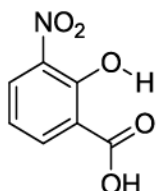
Conditions: CEST data were obtained at 10 mM concentration, pH 7.3 - 7.4, $t_{sat} = 3$ sec, $\omega_1 = 3.6$ μ T and 37 °C.

Table 4

Stereo-electronic effect of 3-substituted 2-hydroxybenzoic acids

Compound	Signal (ppm)	Contrast(%)	k_{ex} (s ⁻¹)
 <p>23</p>	9.5	6.2	240±20
 <p>24</p>	9.3	1.5 ^a	21±5
 <p>25</p>	9.5	7.4	800±200
 <p>26</p>	10.3	6.7	980±90
 <p>27</p>	10.5	9.1	550±40

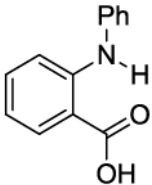
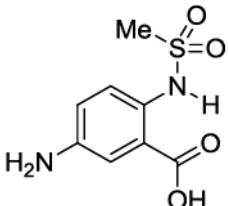
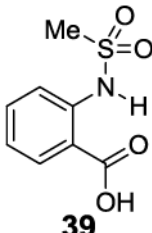
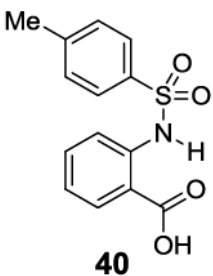
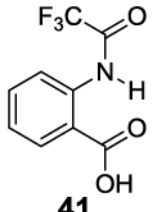
Compound	Signal (ppm)	Contrast(%)	k_{ex} (s^{-1})
 28	10.8	5.3	290±20
 29	10.5	3.4	220±20
 30	10.3	6.4	1400±300
 31	9.0	5.3	2200±200
 32	9.3	6.5	440±50
 33	9.0	6.3	400±20

Compound	Signal (ppm)	Contrast(%)	k_{ex} (s^{-1})
 34	10.5	7.7	520±30
 35	9.5	3.9	7100±400
 36	12.0	5.4	1400±300

Conditions: CEST data were obtained at 10 mM concentration, pH 7.3 - 7.4, $t_{sat} = 3$ sec, $\omega_1 = 3.6$ μ T and 37 °C.

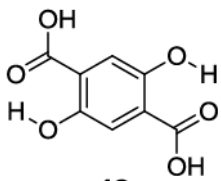
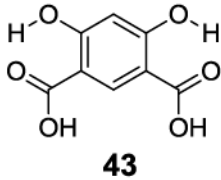
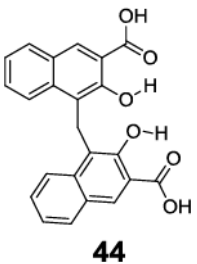
^{a)} 20 mM was used because of the low contrast.

Table 5
Anthranillic acid derivatives as IM-SHY diaCEST probes

Compound	Signal (ppm)	Contrast(%)	k_{ex} (s^{-1})
 <p>37</p>	4.8	7.4	700±40
 <p>38</p>	6.3	8.4	540±30
 <p>39</p>	7.3	7.7	470±30
 <p>40</p>	7.8	6.8	420±30
 <p>41</p>	9.3	3.5	180±20

Conditions: CEST data were obtained at 10 mM concentration, pH 7.3 - 7.4, t_{sat} = 3 sec, ω_1 = 3.6 μ T and 37 °C.

Table 6
Substituted 2-hydroxybenzoic acids with increased IM-SHY signal density

Compound	Signal (ppm)	Contrast(% at 3.6 μ T)	k_{ex} (s^{-1})
 42	8.3	17.1	980 \pm 40
 43	9.8	13.0	460 \pm 30
 44	9.5	5.7	130 \pm 10

Conditions: CEST data were obtained at 10 mM concentration, pH 7.3 - 7.4, t_{sat} = 3 sec, ω_1 = 3.6 μ T and 37 $^{\circ}$ C.